The HopZ Family of *Pseudomonas syringae* Type III Effectors Require Myristoylation for Virulence and Avirulence Functions in *Arabidopsis thaliana*[∇][†]

Jennifer D. Lewis,[1] Wasan Abada,[1] Wenbo Ma,[2] David S. Guttman,[1,3]‡ and Darrell Desveaux[1,3]*‡

Department of Cell & Systems Biology, University of Toronto, 25 Willcocks St., Toronto, Ontario M5S 3B2, Canada[1]; Department of Plant Pathology and Microbiology, University of California, Riverside, 900 University Ave., Riverside, California 92521[2]; and Centre for the Analysis of Genome Evolution & Function, University of Toronto, Toronto, Ontario, Canada[3]

Pseudomonas syringae utilizes the type III secretion system to translocate effector proteins into plant cells, where they can contribute to the pathogen's ability to infect and cause disease. Recognition of these effectors by resistance proteins induces defense responses that typically include a programmed cell death reaction called the hypersensitive response. The YopJ/HopZ family of type III effector proteins is a common family of effector proteins found in animal- and plant-pathogenic bacteria. The HopZ family in *P. syringae* includes HopZ1a$_{PsyA2}$, HopZ1b$_{PgyUnB647}$, HopZ1c$_{PmaE54326}$, HopZ2$_{Ppi895A}$ and HopZ3$_{PsyB728a}$. HopZ1a is predicted to be most similar to the ancestral *hopZ* allele and causes a hypersensitive response in multiple plant species, including *Arabidopsis thaliana*. Therefore, it has been proposed that host defense responses have driven the diversification of this effector family. In this study, we further characterized the hypersensitive response induced by HopZ1a and demonstrated that it is not dependent on known resistance genes. Further, we identified a novel virulence function for HopZ2 that requires the catalytic cysteine demonstrated to be required for protease activity. Sequence analysis of the HopZ family revealed the presence of a predicted myristoylation sequence in all members except HopZ3. We demonstrated that the myristoylation site is required for membrane localization of this effector family and contributes to the virulence and avirulence activities of HopZ2 and HopZ1a, respectively. This paper provides insight into the selective pressures driving virulence protein evolution by describing a detailed functional characterization of the diverse HopZ family of type III effectors with the model plant *Arabidopsis*.

The intimate interaction between plant bacterial pathogens and their hosts is believed to have driven the stepwise evolution of plant resistance mechanisms which successful pathogens have evolved to suppress (11, 18, 28). The gram-negative bacterial phytopathogen *Pseudomonas syringae* uses the type III secretion system to translocate virulence proteins (also known as type III effectors) directly into host cells, where they can suppress host defense responses (1, 9). However, plants have evolved resistance genes that can recognize effectors or the cellular perturbations that they cause and can induce defense responses that can thwart the infection process (15, 40). In fact, certain type III effector genes were originally called avirulence (*avr*) genes due to their ability to compromise the virulence of bacteria that express them. Often associated with the recognition of specific type III effectors by plant resistance proteins is the rapid cell death known as the hypersensitive response (HR), which is localized to the site of infection (23). Recent genome-wide screens have identified hundreds of type III effector proteins in *P. syringae* pathovars that can be sub-

divided into approximately 50 families (35). Although individual effectors have been studied to determine their virulence and/or avirulence functions, detailed analyses of evolutionarily diverse effector families for a specific host are limited (27, 33, 34, 57).

The YopJ/HopZ family is a common and widely distributed class of effector proteins, and members of this family are found in both animal- and plant-pathogenic bacteria. Originally characterized as a cysteine protease (49), the *Yersinia pestis* YopJ protein was recently shown to possess acetyltransferase activity (43, 45). YopJ suppresses the immune response in animals by acetylating serine and threonine residues in the activation loop of members of the mitogen-activated protein kinase kinase superfamily, including MAPKK6, MEK2, and IκB kinase, which prevents their activation by phosphorylation and consequently inhibits their downstream signaling (43, 45, 48). Ma and colleagues recently characterized the HopZ family of YopJ homologues in *P. syringae* and found that three homologues, HopZ1, HopZ2, and HopZ3, were present in ~42% of the 96 strains surveyed from worldwide collections (37). The HopZ family of proteins exhibited weak but significant protease activity when these workers used a fluorescence-based protease assay that was dependent on a conserved cysteine residue that is also found in YopJ (37). It remains to be determined whether the HopZ family also possesses acetyltransferase activity like that demonstrated for YopJ.

HopZ1a$_{PsyA2}$ (formerly HopPsyH), HopZ1b$_{PgyUnB647}$, and HopZ1c$_{PmqES4326}$ (formerly HopPmaD) are closely related al-

lelic variants and form a distinct clade restricted to *P. syringae* (37). HopZ2$_{Ppi895A}$ (formerly AvrPpiG) and HopZ3$_{PsgB728a}$ (formerly HopPsyV) are similar to effectors carried by the plant-pathogenic bacteria *Xanthomonas* spp. and *Erwinia* spp., respectively. These effectors are referred to below as HopZ1a, HopZ1b, HopZ1c, HopZ2, and HopZ3. A detailed evolutionary analysis demonstrated that the HopZ family diversified within the *P. syringae* species complex both by mutational generation of allelic variants (pathoadaptation) and by acquisition of homologs from ecologically similar bacteria via horizontal gene transfer (37). The analysis further showed that the *hopZ1a* allele is most similar to the ancestral *hopZ* allele and that the diversification of the family was most likely driven by the host defense response (37). HopZ1a, HopZ1b, and HopZ2 induce an HR in *Nicotiana benthamiana*, whereas HopZ3 has been demonstrated to induce an HR in snap bean (68) and tobacco (17). In addition, HopZ3 can inhibit the HR induced by AvrPto in *N. benthamiana* (68). Importantly, expression of the ancestral effector HopZ1a in strains carrying degenerate or alternate *hopZ* alleles induces an HR in multiple hosts, including *Arabidopsis thaliana*, while the endogenous HopZ does not (37). The detailed evolutionary characterization of the HopZ family of *P. syringae* type III effectors provides a unique opportunity for examining virulence and avirulence functions in an evolutionary context.

Here, we further characterized the defense response and virulence function of the HopZ family in *Arabidopsis*. We characterized the HopZ1a HR using growth assays, ion leakage assays, and trypan blue staining and showed that it is dependent on myristoylation-mediated membrane localization but independent of the known resistance genes *RPM1*, *RPS2*, *RPS5*, and *RPS4*. In addition, we identified a virulence function for HopZ2 and showed that it is dependent on the catalytic cysteine residue required for in vitro protease activity (37) and also on an intact myristoylation sequence. By thoroughly characterizing the virulence and avirulence functions of the HopZ family in a single host, *Arabidopsis*, in this study we emphasized the functional diversity of the HopZ family of type III effector proteins. This functional diversity of the HopZ proteins likely reflects (i) the diversification of host targets and/or (ii) virulence target modifications by the host surveillance system to avoid recognition.

MATERIALS AND METHODS

Bacterial strains, plasmids, and routine culture conditions. The bacterial strains and plasmids used in this study are listed in Table 1. The following *hopZ* cassettes were cloned from *P. syringae* pathovars: *hopZ1a* from *P. syringae* pv. syringae A2, *hopZ1b* from *P. syringae* pv. glycinea UnB647, *hopZ1c* from *P. syringae* pv. maculicola ES4326, *hopZ2* from *P. syringae* pv. pisi 895A, and *hopZ3* from *P. syringae* pv. syringae B728a (Table 1). *Escherichia coli* and *Agrobacterium tumefaciens* were grown in Luria-Bertani broth, and *P. syringae* was in grown in either King's broth (KB) or minimal medium to induce type III effector expression (24). Antibiotics were used at the following concentrations: for *E. coli*, 50 μg/ml kanamycin; for *A. tumefaciens*, 25 μg/ml gentamicin, 50 μg/ml kanamycin, and 50 μg/ml rifampin; and for *P. syringae*, 50 μg/ml kanamycin, 50 μg/ml rifampin, and 50 μg/ml cycloheximide.

Cloning. Unless otherwise indicated, *Pfu* polymerase (Fermentas) was used for all cloning procedures, and the sequences of all constructs were confirmed by sequencing. All constructs for *Pseudomonas* expression were cloned under their native promoters, with the promoter in the orientation opposite the orientation of the LacZ promoter in the pUCP20 vector (58), and contained an in-frame hemagglutinin (HA) tag at the C terminus. The pUCP20 vector was modified to contain a kanamycin resistance gene in place of the original ampicillin resistance

gene (P. Wang and D. Guttman, unpublished data). The promoters of the *hopZ* genes were defined as starting at the following numbers of nucleotides upstream from the start codon: *hopZ1a*, 182 nucleotides (nt); *hopZ1b*, 237 nt; *hopZ1c*, 236 nt; *hopZ2*, 264 nt; and *hopZ3*, 339 nt from the chaperone. The *hopZ1a* and *hopZ2* genes were amplified by PCR and blunt end cloned into the broad-host-range vector pUCP20, digested with SmaI. The *hopZ1b* and *hopZ1c* genes were amplified by PCR to contain HindIII sites and were cloned into pUCP20. The *hopZ3* gene with the *schZ3* chaperone, designated by using the nomenclature of Lindeberg et al. (35), was amplified by PCR to contain EcoRI sites and was cloned into pUCP20.

To clone C-to-A and G-to-A point mutations, a crossover PCR approach was used (36). The 5′ portion of a gene was amplified by PCR using a 5′ primer to the promoter and a 3′ primer that spanned an ~32-nt region around the desired point mutation. The 3′ portion of the gene was amplified by PCR with a 5′ primer which was the reverse complement of the 3′ primer mentioned above and a 3′ primer to the HA tag. The two PCR products were then mixed and used as a template for the subsequent PCR. The full-length promoter–gene–HA cassette with the desired mutation was amplified using the same 5′ promoter primer and 3′ HA tag primer and cloned into pUCP20 using the sites mentioned above for each *hopZ* gene.

To construct all HopZ-AvrRpt2 fusion proteins, a crossover PCR approach was used (36). For the promoter–full-length *hopZ(G2A)*–HA–*avrRpt2(Δ1–79)* fusions (where G2A indicates a mutation of glycine to alanine in the protein sequence), the 5′ portion of the fusion gene was amplified by PCR using a 5′ primer to the *hopZ* promoter and a 3′ primer to the HA tag plus a portion of the 5′ end of the *avrRpt2* truncation (deletion of amino acids 1 to 79 [Δ1–79]) (21). The 3′ portion of the fusion was amplified by PCR using a 5′ primer to the *avrRpt2* truncation plus a portion of the 3′ end of the HA tag and a 3′ primer to *avrRpt2*. The two PCR products were then mixed and used as a template for the subsequent PCR. The full-length promoter–*hopZ(G2A)*–HA–*avrRpt2(Δ1–79)* cassette was amplified using the same 5′ promoter primer and 3′ *avrRpt2* primer and cloned into pUCP20 as described above. For the promoter-ATG-*avrRpt2(Δ1–79)* fusions, the 5′ portion of the fusion protein was amplified by PCR using a 5′ primer to the *hopZ* promoter and a 3′ primer to the *hopZ* promoter with a start codon and a portion of the 5′ end of *avrRpt2(Δ1–79)*. The 3′ portion of the fusion protein was amplified by PCR using a 5′ primer to the *avrRpt2* truncation plus a start codon and a portion of the 3′ end of the *hopZ* promoter and a 3′ primer to *avrRpt2*. The two PCR products were then mixed and used as a template for the subsequent PCR. The full-length promoter–ATG–*avrRpt2(Δ1–79)* cassette was amplified using the same 5′ promoter primer and 3′ *avrRpt2* primer and cloned into pUCP20 as described above.

To clone into the pBD vector, the *hopZ* genes with an in-frame HA tag were amplified by PCR using primers to add a unique XhoI site to the 5′ end of each gene and a unique SpeI site to the 3′ end of the HA tag. The pBD vector (a gift from Jeff Dangl, University of North Carolina, Chapel Hill) was modified from pTA7002 to add an HA tag in the multiple-cloning site as described previously (2, 39).

***P. syringae* HR, ion leakage, and in planta growth assays.** For infiltration, *P. syringae* was resuspended to an optical density at 600 nm of 0.1 (~5 × 10⁷ CFU/ml) for HR assays and trypan blue staining, diluted to obtain a concentration of 2 × 10⁷ CFU/ml for ion leakage assays, or diluted to obtain a concentration of 1 × 10⁵ CFU/ml for determination of growth curves. Diluted inocula were infiltrated by hand using a needleless syringe as described previously (29). The HR was scored at 16 to 20 h. For trypan blue staining, leaves were harvested after 17 to 18 h and stained with lactophenol-trypan blue (31) by boiling them for 5 min, followed by a 30-min incubation on the bench. Clearing was performed in choral hydrate overnight, and leaves were stored in 60% glycerol. For ion leakage assays, four disks (1.5 cm²) were harvested, soaked in water for 45 min, and transferred to 6 ml of distilled H₂O. Readings were obtained with an Orion 3 Star conductivity meter (Thermo Electron Corporation, Beverly, MA). For growth assays, four disks (1 cm²) were harvested, ground in 10 mM MgCl₂, and plated on KB with rifampin and cycloheximide on days 0 and 3 for colony counting. The chaperone *schZ3* was also present in all *hopZ3* constructs. *Arabidopsis* plants were grown with 9 h of light (~130 microeinsteins m⁻² s⁻¹) and 16 h of darkness at 22°C in Promix soil supplemented with 20:20:20 fertilizer.

***P. syringae* protein expression.** *P. syringae* cultures were grown overnight in KB with kanamycin and rifampin, pelleted, and washed with minimal medium. Cultures were grown overnight in minimal medium to induce the type III secretion system (24). Then, 1.3 ml of each culture was pelleted and resuspended in 50 μl of 1× sodium dodecyl sulfate-polyacrylamide gel electrophoresis (SDS-PAGE) loading dye. Samples were boiled for 5 min. For all proteins except HopZ3, 5 μl of protein was separated on 12% SDS-PAGE gels. For HopZ3 (wild type and mutants), 20 μl was loaded. Proteins were transferred to nitrocellulose mem-

TABLE 1. Strains and plasmids used

Strain or plasmid	Description[b]	Source and/or reference
Strains		
Escherichia coli DH5α	F⁻ φ80Δ*lacZ*ΔM15 Δ(*lacZYA-argF*)U169 *recA1 endA1 hsdR17*(r$_K$⁻ m$_K$⁺) *phoA supE44* λ⁻ *thi-1 gyrA96 relA1*	Invitrogen
Agrobacterium tumefaciens GV3-101	*rpoH*⁺ *hrcA*⁺ C58 ΔpTiC58 Gen^r Rif^r	J. Dangl
Pseudomonas syringae pv. tomato DC3000	Wild type, Rif^r	J. Dangl
Pseudomonas syringae pv. cilantro 0788-9	Wild type, Rif^r	D. Guttman
Pseudomonas syringae pv. syringae A2	Wild type	C. Bender
Pseudomonas syringae pv. glycinea UnB647	Wild type	MAFF[a]
Pseudomonas syringae pv. maculicola ES4326	Wild type	J. Greenberg
Pseudomonas syringae pv. pisi 895A	Wild type	D. Arnold
Pseudomonas syringae pv. syringae B728a	Wild type	S. Hirano
Plasmids		
pUCP20	pUC18-derived broad-host-range vector, Kan^r	D. Guttman
pUCP20-P$_{hopZ1a}$::*hopZ1a*-HA	Native *hopZ1a* promoter (182 nt) drives the *hopZ1a*-HA gene (HA as an in-frame fusion), cloned into the SmaI site	37
pUCP20-P$_{hopZ1b}$::*hopZ1b*-HA	Native *hopZ1b* promoter (237 nt) drives the *hopZ1b*-HA gene (HA as an in-frame fusion), cloned into the HindIII site	This study
pUCP20-P$_{hopZ1c}$::*hopZ1c*-HA	Native *hopZ1c* promoter (236 nt) drives the *hopZ1c*-HA gene (HA as an in-frame fusion), cloned into the HindIII site	This study
pUCP20-P$_{hopZ2}$::*hopZ2*-HA	Native *hopZ2* promoter (264 nt) drives the *hopZ2*-HA gene (HA as an in-frame fusion), cloned into the SmaI site	This study
pUCP20-P$_{hopZ3}$::*schZ3-hopZ3*-HA	Native *hopZ3* promoter (339 nt) drives the *schZ3-hopZ3*-HA gene (HA as an in-frame fusion), cloned into the EcoRI site	This study
pUCP20-P$_{hopZ1a}$::*hopZ1a(C216A)*-HA	Native *hopZ1a* promoter (182 nt) drives the *hopZ1a(C216A)*-HA gene (HA as in-frame fusion), cloned into the SmaI site	This study
pUCP20-P$_{hopZ1b}$::*hopZ1b(C212A)*-HA	Native *hopZ1b* promoter (237 nt) drives the *hopZ1b(C212A)*-HA gene (HA as an in-frame fusion), cloned into the HindIII site	This study
pUCP20-P$_{hopZ1c}$::*hopZ1c(C212A)*-HA	Native *hopZ1c* promoter (236 nt) drives the *hopZ1c(C212A)*-HA gene (HA as an in-frame fusion), cloned into the HindIII site	This study
pUCP20-P$_{hopZ2}$::*hopZ2(C229A)*-HA	Native *hopZ2* promoter (264 nt) drives the *hopZ2(C229A)*-HA gene (HA as an in-frame fusion), cloned into the SmaI site	This study
pUCP20-P$_{hopZ3}$::*schZ3-hopZ3(C300A)*-HA	Native *hopZ3* promoter (339 nt) drives the *schZ3-hopZ3(C300A)*-HA gene (HA as an in-frame fusion), cloned into the EcoRI site	This study
pUCP20-P$_{hopZ1a}$::*hopZ1a(G2A)*-HA	Native *hopZ1a* promoter (182 nt) drives the *hopZ1a(G2A)*-HA gene (HA as an in-frame fusion), cloned into the SmaI site	This study
pUCP20-P$_{hopZ1b}$::*hopZ1b(G2A)*-HA	Native *hopZ1b* promoter (237 nt) drives the *hopZ1b(G2A)*-HA gene (HA as an in-frame fusion), cloned into the HindIII site	This study
pUCP20-P$_{hopZ1c}$::*hopZ1c(G2A)*-HA	Native *hopZ1c* promoter (236 nt) drives the *hopZ1c(G2A)*-HA gene (HA as an in-frame fusion), cloned into the HindIII site	This study
pUCP20-P$_{hopZ2}$::*hopZ2(G2A)*-HA	Native *hopZ2* promoter (264 nt) drives the *hopZ2(G2A)*-HA gene (HA as an in-frame fusion), cloned into the SmaI site	This study
pUCP20-P$_{hopZ1a}$::*hopZ1a(G2A)*-HA-*avrRpt2*(Δ1–79)	Native *hopZ1a* promoter (182 nt) drives the *hopZ1a(G2A)*-HA-*avrRpt2*(Δ1–79) gene (HA and *avrRpt2* as an in-frame fusion), AvrRpt2 lacks its normal secretion and translocation sequence (amino acids 1 to 79), cloned into the SmaI site	This study
pUCP20-P$_{hopZ2}$::*hopZ2(G2A)*-HA-*avrRpt2*(Δ1–79)	Native *hopZ2* promoter (264 nt) drives the *hopZ2(G2A)*-HA-*avrRpt2*(Δ1–79) gene (HA and *avrRpt2* as an in-frame fusion), AvrRpt2 lacks its normal secretion and translocation sequence (amino acids 1 to 79), cloned into the SmaI site	This study
pUCP20-P$_{hopZ1a}$::*ATG-avrRpt2*(Δ1–79)	Native *hopZ1a* promoter (182 nt) drives the ATG-*avrRpt2*(Δ1–79) gene, AvrRpt2 lacks its normal secretion and translocation sequence (amino acids 1 to 79), cloned into the SmaI site	This study
pUCP20-P$_{hopZ2}$::*ATG-avrRpt2*(Δ1–79)	Native *hopZ2* promoter (264 nt) drives the ATG-*avrRpt2*(Δ1–79) gene, AvrRpt2 lacks its normal secretion and translocation sequence (amino acids 1 to 79), cloned into the SmaI site	This study
pDSK519-P$_{nptII}$::*avrRpt2*	*nptII* promoter drives *avrRpt2* gene expression, Kan^r	44; J. Dangl

Continued on following page

TABLE 1—*Continued*

Strain or plasmid	Description[b]	Source and/or reference
pBD	Modified from pTA7002 to have an HA tag in the multiple cloning site; dexamethasone-inducible expression and BASTA^r in plants, Kan^r in bacteria	2; J. Dangl
pBD::*hopZ1a*-HA	Coding sequence of the *hopZ1a* gene with in-frame HA cloned into the XhoI and SpeI sites	This study
pBD::*hopZ1b*-HA	Coding sequence of the *hopZ1b* gene with in-frame HA cloned into the XhoI and SpeI sites	This study
pBD::*hopZ1c*-HA	Coding sequence of the *hopZ1c* gene with in-frame HA cloned into the XhoI and SpeI sites	This study
pBD::*hopZ2*-HA	Coding sequence of the *hopZ2* gene with in-frame HA cloned into the XhoI and SpeI sites	This study
pBD::*hopZ3*-HA	Coding sequence of the *hopZ3* gene with in-frame HA cloned into the XhoI and SpeI sites	This study
pBD::*hopZ1a*(*G2A*)-HA	Coding sequence of the *hopZ1a*(*G2A*) gene with in-frame HA cloned into the XhoI and SpeI sites	This study
pBD::*hopZ1b*(*G2A*)-HA	Coding sequence of the *hopZ1b*(*G2A*) gene with in-frame HA cloned into the XhoI and SpeI sites	This study
pBD::*hopZ1c*(*G2A*)-HA	Coding sequence of the *hopZ1c*(*G2A*) gene with in-frame HA cloned into the XhoI and SpeI sites	This study
pBD::*hopZ2*(*G2A*)-HA	Coding sequence of the *hopZ2*(*G2A*) gene with in-frame HA cloned into the XhoI and SpeI sites	This study

[a] MAFF, Japanese Ministry of Agriculture, Forestry and Fisheries.
[b] nt, nucleotide; BASTA, glufosinate ammonium.

branes and detected with HA antibodies (Roche) by chemiluminescence (Amersham Biosciences).

***Agrobacterium* transient-expression assays and membrane fractionation.** Five-milliliter *A. tumefaciens* GV3-101 cultures were grown overnight at 28°C in Luria-Bertani broth with gentamicin, kanamycin, and rifampin. The following day, the cultures were washed twice in induction medium (50 mM morpholineethanesulfonic acid [MES] [pH 5.6], 0.5% [wt/vol] glucose, 1.7 mM NaH_2PO_4, 20 mM NH_4Cl, 1.2 mM $MgSO_4$, 2 mM KCl, 17 μM $FeSO_4$, 70 μM $CaCl_2$, 200 μM acetosyringone) (59), and 3.2 ml of each culture was inoculated into 50 ml of fresh induction medium and grown overnight. The following day, the cultures were spun down, washed twice in 10 mM MES (pH 5.6) with 200 μM acetosyringone, and infiltrated at an optical density at 600 nm of 0.3 into the undersides of leaves of 5- to 7-week-old *N. benthamiana* plants. The plants were sprayed with 20 μM dexamethasone (Sigma) 5 to 6 h after inoculation. Then, 1 cm^2 of leaf tissue was harvested at 21 to 24 h after dexamethasone induction and frozen in liquid nitrogen. The leaf tissue was ground in a buffer containing 20 mM Tris (pH 8.0), 1 mM EDTA (pH 8.0), 1 mM dithiothreitol, and 0.33 M sucrose. The crude extract was cleared by centrifugation at $5,000 \times g$ for 10 min at 4°C. To separate soluble and membrane proteins, the cleared extract was centrifuged at $20,000 \times g$ for 1 h at 4°C. After SDS-PAGE loading dye was added to equivalent volumes of soluble and membrane fractions and the preparations were boiled for 5 min, 7.5 μl of protein was separated on 12% SDS-PAGE gels, blotted onto nitrocellulose membranes, and detected using HA antibodies (Roche) by chemiluminescence (Amersham Biosciences).

Computer software. The sequence analysis was done with BioEdit 7.0 and Sequencer 4.0. Adobe Photoshop 7.0 was used for all image manipulation. Statview 5.0 was used for all statistical analyses.

RESULTS

Characterization of the HopZ1a-induced HR in *Arabidopsis*. Ma and colleagues (37) previously noted that HopZ1a induces an HR in *Arabidopsis* ecotype Col-0 plants when it is expressed in *P. syringae* pv. maculicola ES4326, a virulent strain of *P. syringae* which also carries HopZ1c. To further investigate HopZ-induced HR in *Arabidopsis*, we expressed the individual *hopZ* alleles using their native promoters in *P. syringae* pv. tomato DC3000, which is also a virulent strain on *Arabidopsis* but does not carry any endogenous *hopZ* genes. *Arabidopsis* ecotype Col-0 leaves were infected with *P. syringae* pv. tomato

DC3000 expressing HopZ1a, HopZ1b, HopZ1c, HopZ2, HopZ3, AvrRpt2, or the empty vector pUCP20 and monitored for macroscopic HR-like symptoms. *P. syringae* pv. tomato DC3000 expressing HopZ1a induced an HR in *Arabidopsis* ecotype Col-0 that was observed about 22 h postinfection. This timing is similar to the timing of the *RPS2*-mediated HR induced by AvrRpt2 (Fig. 1A) (52). The catalytic cysteine of HopZ1a (C216) was required for the HR, since a cysteine-to-alanine mutation in this amino acid [HopZ1a(C216A)] abrogated the HR. HopZ1c, HopZ2, and HopZ3 were never observed to induce a macroscopic HR. However, HopZ1b triggered a weak HR in 24% (11/45) of the plants. The HopZ1b-induced HR was delayed about 2 h relative to the HR induced by HopZ1a. The lack of an HR was not due to a lack of protein expression in *P. syringae* pv. tomato DC3000 since all alleles were detected by Western blotting (Fig. 1B). As another qualitative measure of the HR, we used trypan blue staining (Fig. 1C). Leaves infiltrated with *P. syringae* pv. tomato DC3000 expressing the *hopZ* alleles or the empty pUCP20 vector were stained with trypan blue 18 h postinfection. Cell death associated with the HR induced by HopZ1a and AvrRpt2 was indicated by heavy trypan blue staining. This result was in contrast to the results for leaves infiltrated with *P. syringae* pv. tomato DC3000 expressing HopZ1a(C216A), HopZ1b, HopZ1c, HopZ2, or HopZ3, which were not stained significantly with trypan blue.

As a quantitative measure of the HR, we monitored the leakage of ions into the medium and the resulting changes in conductivity over time (Fig. 1D). *Arabidopsis* ecotype Col-0 leaves infiltrated with *P. syringae* pv. tomato DC3000 expressing HopZ1a exhibited a rapid loss of ions detectable at 10 h postinfection, and the level plateaued at about 16 h postinfection. This response was slightly slower than the response observed for leaves infiltrated with *P. syringae* pv. tomato DC3000 expressing AvrRpt2, in which a plateau was
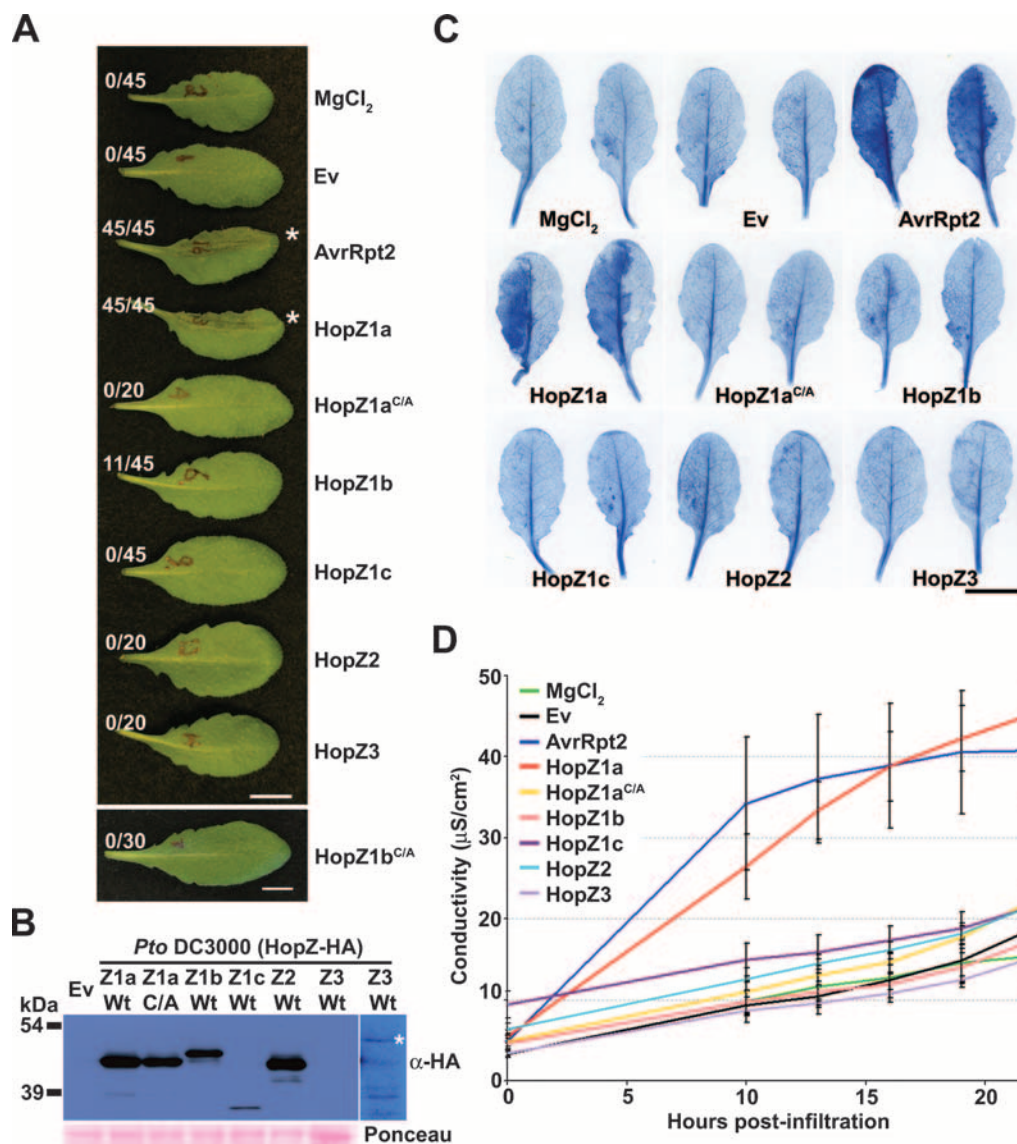
FIG. 1. Characterization of the HR induced by HopZ1a in *Arabidopsis*. (A) Half-leaves of *Arabidopsis* plants were infiltrated with 10 mM MgCl$_2$ or with *P. syringae* pv. tomato DC3000 expressing the empty vector (Ev) or one of the HopZ family members with a C-terminal HA tag under the control of its endogenous promoter. The bacteria (5×10^7 CFU/ml) were syringe infiltrated into the leaves. Photographs were taken 22 h after infiltration. The numbers of leaves showing an HR are indicated to the left of the leaves. HRs are indicated by an asterisk. HopZ1a$^{C/A}$, C216A mutant; HopZ1b$^{C/A}$, C212A mutant (the picture was taken in a separate experiment). Scale bars = 1 cm. (B) Immunoblot analysis of HopZ-HA family protein expression in *P. syringae* pv. tomato DC3000. *P. syringae* pv. tomato DC3000 (*Pto* DC3000) carrying an empty vector or one of the indicated HA-tagged HopZ proteins was grown in minimal medium to induce the type III secretion system. Equal amounts of protein were resolved on 12% SDS-PAGE gels, blotted onto nitrocellulose, and probed with HA antibodies. The darkest band in each lane is the band corresponding to the full-length HopZ-HA protein. Other bands are nonspecific or degradation products. The Ponceau red-stained blot was used as a loading control. The HopZ3 lane was loaded with four times as much protein as was in the other lanes, and the additional HopZ3 panel on the right shows an overexposure (10×) of the same blot. The HopZ3 band is indicated by an asterisk. The molecular masses of the proteins are as follows: HopZ1a-HA, 42.1 kDa; HopZ1b-HA, 42.4 kDa; HopZ1c-HA, 30.5 kDa; HopZ2-HA, 41.9 kDa; and HopZ3-HA, 46.9 kDa. C/A, C216A mutant; Wt, wild type; α-HA, anti-HA. (C) Trypan blue staining of *P. syringae* pv. tomato DC3000-infiltrated *Arabidopsis* leaves. The bacteria (5×10^7 CFU/ml) were syringe infiltrated into the leaves. C/A, C216A mutant of HopZ1a. Scale bar = 1 cm. (D) Electrolyte leakage of *Arabidopsis* leaf disks after infiltration with *P. syringae* pv. tomato DC3000 expressing the indicated constructs. The bacteria were syringe infiltrated into the leaves using a suspension containing 2×10^7 CFU/ml. The error bars indicate the standard deviations from four repetitions. C/A, C216A mutant.

reached by 10 h postinfection. Leaves infiltrated with *P. syringae* pv. tomato DC3000 expressing HopZ1a(C216A) showed a level of ion leakage similar to that of leaves infiltrated with bacteria expressing the empty vector. Consistent with the macroscopic HR phenotypes, *P. syringae* pv. tomato

DC3000 expressing HopZ1b, HopZ1c, HopZ2, and HopZ3 increased conductivity similarly to bacteria expressing the empty pUCP20 vector.

Contribution of the HopZ family to *P. syringae* growth in *Arabidopsis*. To examine the contribution of the HopZ family to
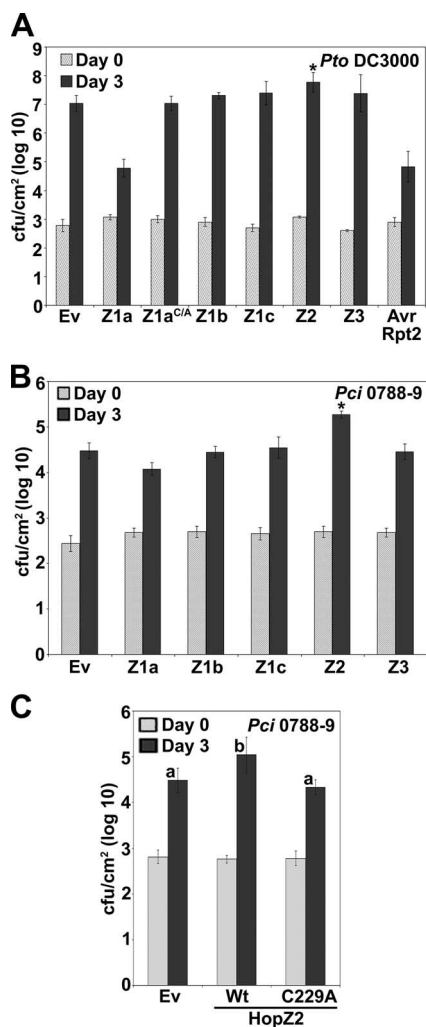
FIG. 2. Avirulence and virulence functions of the HopZ family in *Arabidopsis*. (A) *P. syringae* pv. tomato DC3000 (*Pto* DC3000) expressing the indicated HopZ-HA family members was syringe infiltrated using a suspension containing 1×10^5 CFU/ml into *Arabidopsis* ecotype Col-0 leaves, and bacterial counts were determined 1 h postinfection (day 0) and 3 days postinfection (day 3). Z1a$^{C/A}$, C216A mutant of HopZ1a; Ev, empty vector. (B) *P. syringae* pv. cilantro 0788-9 (*Pci* 0788-9) expressing the indicated HopZ-HA family members was syringe infiltrated using a suspension containing 1×10^5 CFU/ml into *Arabidopsis* ecotype Col-0 leaves, and bacterial counts were determined 1 h postinfection (day 0) and 3 days postinfection (day 3). (C) Bacterial growth of *P. syringae* pv. cilantro 0788-9 expressing the empty vector, HopZ2-HA (wild type [Wt]), and the HopZ2-HA(C229A) mutant as described above. Asterisks indicate values significantly different from the value for the empty vector control according to Fisher's PLSD test. The error bars indicate 1 standard deviation from the mean. The letters above the bars indicate significance groups.

bacterial growth in *Arabidopsis* ecotype Col-0, we carried out growth assays with *P. syringae* pv. tomato DC3000 expressing the five *hopZ* alleles individually. Bacteria were syringe infiltrated (29) into the leaves of ecotype Col-0 plants, and the bacterial levels were monitored at 1 h (day 0) and 3 days postinfection. The growth of *P. syringae* pv. tomato DC3000 expressing HopZ1a was reduced more than 100-fold compared to the growth of *P. syringae* pv. tomato DC3000 harboring the empty vector at 3 days postin-

fection (Fig. 2A). The reduction in bacterial growth was similar to the reduction in the *RPS2*-mediated resistance induced by Avr-Rpt2 (Fig. 2A). Therefore, the HopZ1a-induced HR in *Arabidopsis* ecotype Col-0 is associated with a decrease in bacterial growth. Like the macroscopic HR, HopZ1a-induced resistance requires the catalytic cysteine since *P. syringae* pv. tomato DC3000 expressing HopZ1a(C216A) grew as well as *P. syringae* pv. tomato DC3000 expressing the empty vector (Fig. 2A).

In contrast to HopZ1a, HopZ2 conferred a significant growth advantage to *P. syringae* pv. tomato DC3000 in planta ($P = 0.0002$, Fisher's protected least significant difference [PLSD] post hoc test). Since *P. syringae* pv. tomato DC3000 is a relatively strong pathogen of *Arabidopsis*, we wanted to confirm the growth advantage conferred by HopZ2 in a weaker *Arabidopsis* pathogen. We transformed HopZ2 constructs into *P. syringae* pv. cilantro 0788-9, which grows very poorly in *Arabidopsis* ecotype Col-0 despite the fact that it is closely related to *P. syringae* pv. maculicola ES4326, which is virulent on *Arabidopsis* (25, 37, 56). Expression of HopZ2 in *P. syringae* pv. cilantro 0788-9 increased the growth by 0.5 to 0.75 order of magnitude compared to the growth of *P. syringae* pv. cilantro 0788-9 carrying the empty pUCP20 vector ($P < 0.0001$, Fisher's PLSD post hoc test) (Fig. 2B). HopZ2(C229A) did not confer a growth advantage to *P. syringae* pv. cilantro 0788-9 ($P = 0.897$), demonstrating that the catalytic residue is required for the HopZ2 virulence function (Fig. 2B and C). None of the other HopZ family members significantly enhanced *P. syringae* pv. cilantro 0788-9 growth in *Arabidopsis* (Fig. 2B). Differences in growth were not due to a lack of expression since all proteins were expressed at similar levels in *P. syringae* pv. cilantro 0788-9 (see Fig. S1 in the supplemental material). Therefore, of the five HopZ family members examined to determine their effects on bacterial growth in *Arabidopsis*, HopZ1a induced an HR that compromised bacterial growth, whereas HopZ2 promoted bacterial growth. Both activities required the cysteine residues previously demonstrated to be required for protease activity in vitro (37).

HopZ1a-induced HR is not dependent on *RPM1*, *RPS2*, *RIN4*, *RPS5*, or *RPS4*. To determine whether the HR induced by HopZ1a is dependent on previously characterized resistance genes or the resistance protein-associated protein RIN4 (*RPM1-in*teracting protein 4) (4, 39), we carried out macroscopic HR assays or growth assays with *Arabidopsis* plants lacking these genes. The activities of AvrB and AvrRpm1 are recognized by *RPM1* (20), while the activity of AvrRpt2 is recognized by *RPS2* (6, 42). *Arabidopsis rpm1-3 rps2-101C rin4* (5) leaves were infected with *P. syringae* pv. tomato DC3000 expressing HopZ1a, HopZ1a(C216A), AvrRpt2, or the empty vector pUCP20 and monitored for macroscopic HR-like symptoms. Since AvrRpt2 recognition is dependent on *RIN4* and *RPS2* in *Arabidopsis*, the disruption of these genes impaired the HR normally caused by AvrRpt2 (Fig. 3A). HopZ1a still induced an HR in the *rpm1-3 rps2-101C rin4* mutant background (Fig. 3A), indicating that it is not recognized by the resistance protein RPM1 or RPS2 or by the RPM1-interacting protein RIN4. Consistent with our previous data, the catalytic cysteine residue in HopZ1a was necessary for the HopZ1a-induced HR (Fig. 3A). We also tested an *rps5-2* mutant in which the *RPS5* resistance gene required for the recognition of HopAR1 (AvrPphB) is impaired (62). *Arabidopsis rps5-2* mutant leaves were infected with *P. syringae* pv. tomato DC3000
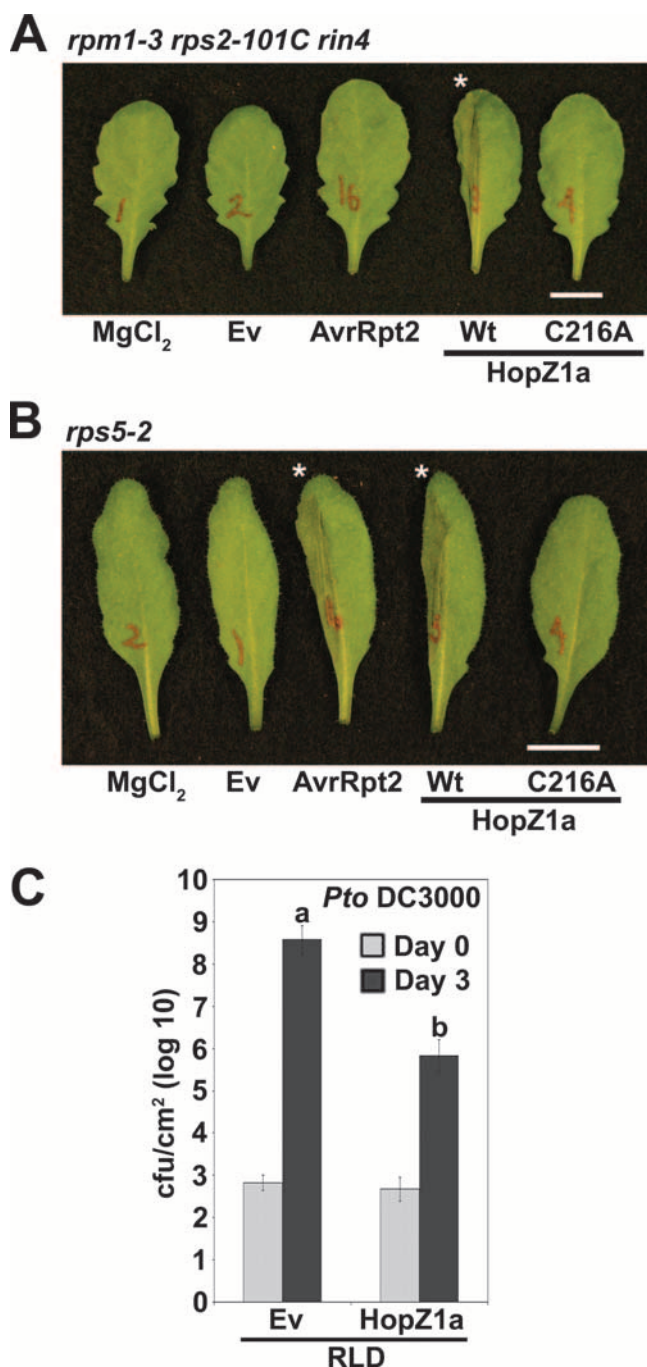
FIG. 3. HopZ1a-induced HR in *Arabidopsis* is independent of *RPM1*, *RPS2*, *RIN4*, *RPS5*, and *RPS4*. (A) Half-leaves of *Arabidopsis rpm1-3 rps2-101C rin4* plants were infiltrated with 10 mM MgCl₂ or with *P. syringae* pv. tomato DC3000 expressing the empty vector, AvrRpt2, or HopZ1a with a C-terminal HA tag under the control of its endogenous promoter. The bacteria (5×10^7 CFU/ml) were syringe infiltrated into the leaves. Photographs were taken 22 h after infiltration. An HR is indicated by an asterisk. Ev, empty vector; Wt, wild type; C216A, C216A mutant. Scale bar = 1 cm. (B) Half-leaves of *Arabidopsis rps5-2* plants were infiltrated as described for panel A. Scale bar = 1 cm. (C) *P. syringae* pv. tomato DC3000 (*Pto* DC3000) expressing HopZ1a-HA or the empty vector was syringe infiltrated into *Arabidopsis* ecotype RLD leaves, and bacterial counts were determined 1 h postinfection (day 0) and 3 days postinfection (day 3). The bacteria (1×10^5 CFU/ml) were syringe infiltrated into the leaves. The error bars indicate 1 standard deviation from the mean. The letters above the bars indicate significance groups according to Fisher's PLSD test.

TABLE 2. Members of the HopZ family contain an N-myristoylation consensus sequence

Protein(s)	Amino acid at position:									Reference
	1	2	3	4	5	6	7	8	9	
AvrB	M	G	C	V	S	S	K	S	T	46
HopAR1[a]		G	C	A	S	S	G	V	S	46
AvrRpm1	M	G	C	V	S	S	T	S	R	46
AvrC	M	G	N	V	C	F	R	P	S	63
AvrPto	M	G	N	I	C	V	G	G	S	60
HopZ1a	M	G	N	V	C	V	G	G	S	37
HopZ1b and HopZ1c[b]	M	G	N	I	C	I	G	G	P	37
HopZ2[c]	M	G	I	C	V	S	K	P	S	37
HopZ3	M	N	I	S	G	P	N	R	R	37

[a] Internal cleavage of HopAR1 (AvrPphB) revealed the myristoylated glycine at the N terminus (46, 50).
[b] Previously described by Maurer-Stroh and Eisenhaber (41).
[c] Previously described by Thieme et al. (65).

expressing HopZ1a, HopZ1a(C216A), AvrRpt2, or an empty vector and monitored for macroscopic HR-like symptoms. HopZ1a still induced an HR in the *rps5-2* mutant, which indicated that *RPS5* does not have a role in the HR conferred by HopZ1a (Fig. 3B).

We also tested a naturally occurring susceptible ecotype, ecotype RLD, which is susceptible to *P. syringae* pv. tomato DC3000 carrying AvrRps4 and lacks a functional *RPS4* gene (19). Since this resistance gene can induce resistance in *Arabidopsis* without an associated HR (19), we tested ecotype RLD to determine whether there was a reduction in bacterial growth when it was infiltrated with *P. syringae* pv. tomato DC3000 carrying HopZ1a. Bacteria were syringe infiltrated into the leaves of ecotype RLD plants, and the bacterial levels were monitored at 1 h (day 0) and 3 days postinfection. The growth of *P. syringae* pv. tomato DC3000 expressing HopZ1a was reduced more than 100-fold compared to the growth of *P. syringae* pv. tomato DC3000 harboring the empty pUCP20 vector at 3 days postinfection in the RLD ecotype (Fig. 3C). The reduction in bacterial growth was similar to that observed for ecotype Col-0 (Fig. 2A). Thus, *RPS4* is not required for the HopZ1a-induced HR.

Members of the HopZ family contain a putative myristoylation site required for membrane localization in planta. Myristoylation is the irreversible attachment of a myristoyl group to the N-terminal glycine residue of proteins that can act as a lipid anchor in biological membranes (8). Several bacterial type III effector proteins contain predicted myristoylation sequences at their N termini (Table 2) (41, 46). AvrB and AvrRpm1 have been demonstrated to be myristoylated in vivo and to require this modification for avirulence functions in planta (46). Putative myristoylation sites have also been found in the HopZ1c and HopZ2 proteins (41, 65). When we analyzed the N-terminal regions of the HopZ proteins, we noticed that the sequence of HopZ1a is nearly identical to that of AvrPto, except for one conservative amino acid difference, and is very similar to those of HopZ1b and HopZ1c (Table 2). HopZ2 is more divergent, although it retains a glycine at the second position. HopZ3 does not appear to have a consensus sequence for myristoylation (data not shown). This suggested that all of the HopZ family members except HopZ3 may be membrane associated in planta.
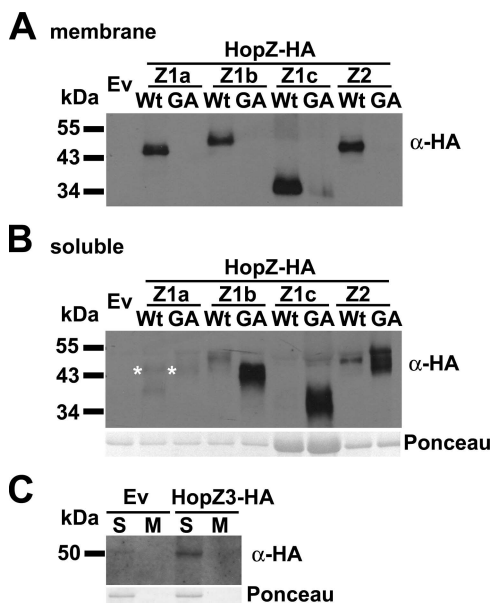
FIG. 4. HopZ1a, HopZ1b, HopZ1c, and HopZ2 possess a predicted myristoylation consensus sequence that is required for membrane localization in *N. benthamiana*. (A) Membrane fractions from 1-cm^2 sectors of *N. benthamiana* leaves syringe infiltrated with *Agrobacterium* carrying the indicated constructs in a conditional dexamethasone-inducible expression vector (as described in Materials and Methods). Proteins were resolved on 12% SDS-PAGE gels, blotted onto nitrocellulose, and probed with HA antibodies (α-HA). The predicted molecular masses of the proteins are as follows: HopZ1a-HA, 42.1 kDa; HopZ1b-HA, 42.4 kDa; HopZ1c-HA, 30.5 kDa; and HopZ2-HA, 41.9 kDa. Equivalent proportions of proteins were loaded for the membrane and soluble fractions. Ev, empty vector; GA, G2A mutant; Wt, wild type. (B) Immunoblot analysis of the soluble fraction of the extract used for panel A. Cellular equivalents of the membrane fraction in panel A and the soluble fraction in panel B were loaded (as described in Materials and Methods). Asterisks to the left of the lanes for HopZ1a and HopZ1a(G2A) indicate the band of interest. Ponceau red staining demonstrated that equal amounts of protein were loaded for the empty vector, HopZ1a, HopZ1a(G2A), HopZ1b, HopZ1b(G2A), HopZ2, and HopZ2(G2A) and that five times more protein was loaded for HopZ1c and HopZ1c(G2A). (C) Membrane (M) and soluble (S) fractions for the empty vector and HopZ3. Ponceau red staining demonstrated that equal amounts of protein were loaded for the empty vector and HopZ3. The autoradiograph was overexposed 20 times relative to those in panels A and B. The predicted molecular mass of HopZ3-HA is 46.9 kDa.

To examine the localization of the HopZ family proteins in planta, we expressed them in *N. benthamiana* under a dexamethasone-inducible promoter by using *Agrobacterium*-mediated transient expression. Membrane localization was determined by protein fractionation and Western blot analysis. Dexamethasone-expressed HopZ1a, HopZ1b, and HopZ2 induced an HR (data not shown), as observed previously with constitutively expressed HopZ proteins (37). As predicted from the sequence data in Table 2, HopZ1a, HopZ1b, HopZ1c, and HopZ2 were detected mainly in the membrane fraction upon overexpression in planta, while HopZ3 was detected only in the soluble fraction (Fig. 4). Some HopZ1a, HopZ1b, HopZ1c, and HopZ2 proteins were also weakly detected in the soluble fraction, but the abundance was much lower than that of the membrane-associated protein (Fig. 4A and B), possibly due to overex-

pression by dexamethasone. While the expression level of HopZ3 was always quite low, we never observed HopZ3 protein in the membrane fraction (Fig. 4C). To determine if the predicted myristoylation sequences of members of the HopZ family are involved in membrane association, we changed the conserved glycine residue at the N termini of HopZ1a, HopZ1b, HopZ1c, and HopZ2 to alanine (Table 2 and Fig. 4). The wild-type and mutant G2A proteins were expressed in *N. benthamiana* using agroinfiltration, and proteins were fractionated and detected by Western blot analysis. Unlike the wild-type proteins, HopZ1a(G2A), HopZ1b(G2A), HopZ1c(G2A), and HopZ2(G2A) were detected mainly in the soluble fraction (Fig. 4A and B). The expression of HopZ1a(G2A) was lower than that of the wild-type HopZ1a protein (Fig. 4A and 4B), but this protein was still clearly visible in the soluble fraction. These experiments demonstrated that HopZ1a, HopZ1b, HopZ1c, and HopZ2, but not HopZ3, are predominantly membrane localized when they are overexpressed in planta. Furthermore, the glycine residue at position 2 is required for membrane localization, strongly suggesting that myristoylation contributes to the localization of these proteins to membranes.

Myristoylation contributes to the avirulence and virulence functions of HopZ1a and HopZ2. To test whether membrane localization is required for HopZ function, we examined the effects of mutating the putative myristoylation sequence on HopZ1a and HopZ2 avirulence and virulence functions. *P. syringae* pv. tomato DC3000 expressing HopZ1a(G2A) was infiltrated into *Arabidopsis* leaves, and the leaves were examined for development of an HR. Unlike wild-type HopZ1a, HopZ1a(G2A) did not induce an HR in *Arabidopsis* ecotype Col-0 plants (Fig. 5A). The lack of an HR was not due to lack of expression since Western blot analysis revealed that HopZ1a(G2A) was expressed at levels comparable to those of wild-type HopZ1a in *P. syringae* pv. tomato DC3000 (Fig. 5B). The G2A mutation also had no effect on translocation through the type III secretion system because a chimeric fusion of the full-length HopZ1a(G2A) protein to the C terminus of AvrRpt2 (amino acids 80 to 255) (21) induced an HR in *Arabidopsis* (see Fig. S2 in the supplemental material). Staining of infected leaves with trypan blue confirmed the lack of HR cell death induction by HopZ1a(G2A) compared to the effect of wild-type HopZ1a (Fig. 5C). Ion leakage assays (Fig. 5D) corroborated the qualitative HR data, since *P. syringae* pv. tomato DC3000 expressing HopZ1a(G2A) caused ion leakage from leaf disks similar to that caused by *P. syringae* pv. tomato DC3000 carrying the empty vector. To examine whether the G2 residue is required for HopZ1a-mediated resistance, we carried out growth assays with *P. syringae* pv. tomato DC3000 containing wild-type HopZ1a and HopZ1a(G2A). *P. syringae* pv. tomato DC3000 carrying HopZ1a grew approximately 1,000-fold less than *P. syringae* pv. tomato DC3000 carrying the empty vector, as previously observed (Fig. 2A). *P. syringae* pv. tomato DC3000 carrying HopZ1a(G2A) showed intermediate growth [the growth was about 10-fold less than the growth of *P. syringae* pv. tomato DC3000 carrying the empty vector or HopZ1a(C216A)] but grew about 100-fold more than *P. syringae* pv. tomato DC3000 expressing wild-type HopZ1a (Fig. 5E). This implies that the
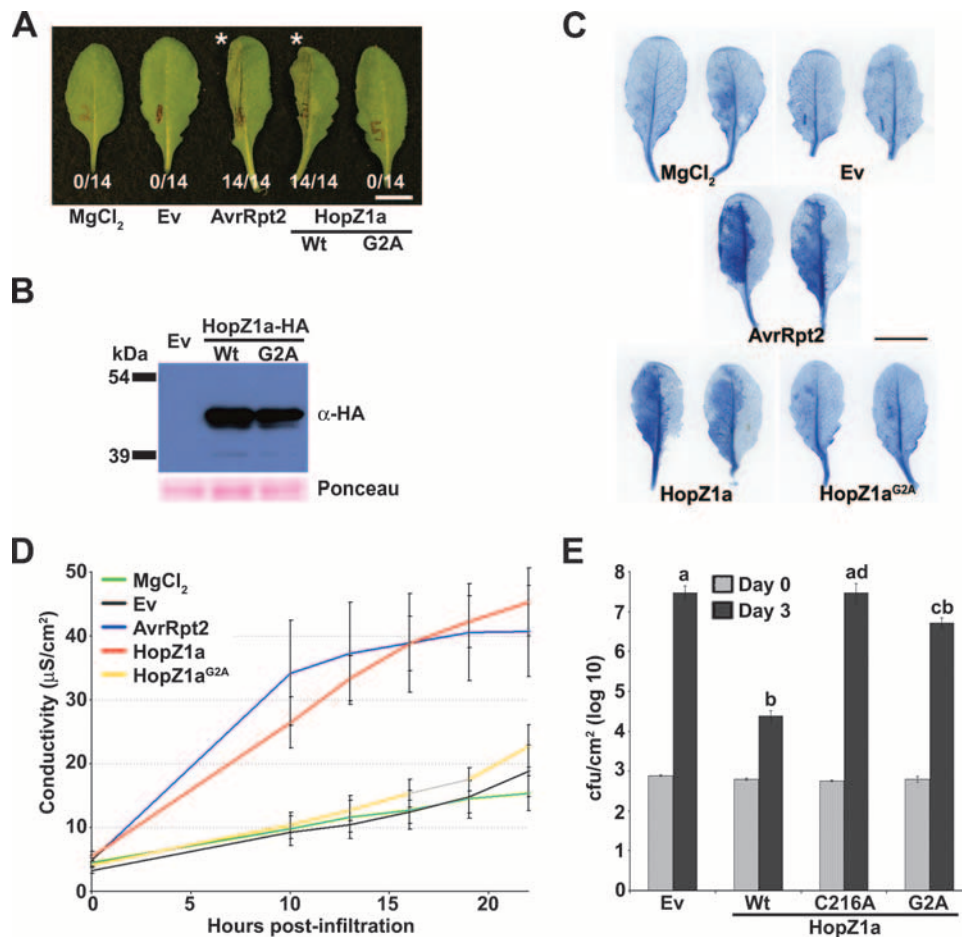
FIG. 5. Myristoylation site of HopZ1a is required for the induction of the HR and contributes to associated defenses. (A) Half-leaves of *Arabidopsis* ecotype Col-0 plants were mock infiltrated with 10 mM MgCl$_2$ or syringe infiltrated with *P. syringae* pv. tomato DC3000 carrying the empty vector or a member of the HopZ family with a C-terminal HA tag under the control of its endogenous promoter. The bacteria (5×10^7 CFU/ml) were syringe infiltrated into the leaves. The photographs were taken 22 h after infiltration. Ev, empty vector; Wt, wild type; G2A, G2A mutant. Scale bar = 1 cm. (B) Immunoblot analysis of HopZ1a-HA proteins in *P. syringae* pv. tomato DC3000. Equal amounts of protein were loaded. The molecular mass of HopZ1a-HA is 42.1 kDa. (C) Trypan blue staining of DC3000-infiltrated *Arabidopsis* leaves. The bacteria (5×10^7 CFU/ml) were syringe infiltrated into the leaves. Scale bar = 1 cm. (D) Electrolyte leakage after infiltration with the indicated constructs. The bacteria (2×10^7 CFU/ml) were syringe infiltrated into the leaves. The error bars indicate the standard deviations for four repetitions. (E) *P. syringae* pv. tomato DC3000 carrying the indicated constructs was syringe infiltrated into *Arabidopsis* ecotype Col-0 leaves, and bacterial counts were determined on days 0 and 3. The bacteria (1×10^5 CFU/ml) were syringe infiltrated into the leaves. The error bars indicate 1 standard deviation from the mean. Fisher's PLSD test was used to assess significance. The letters above the bars indicate significance groups.

lack of myristoylation weakens but does not eliminate HopZ1a-induced defense responses. These data, together with the results of our membrane fractionation experiments (Fig. 4), indicate that the membrane localization of HopZ1a contributes to the recognition of this effector by *Arabidopsis* ecotype Col-0 and the subsequent establishment of an HR and associated defense responses. Finally, we examined whether the predicted myristoylation site is required for HopZ2 virulence function (Fig. 6). Unlike the expression of wild-type HopZ2, the expression of HopZ2(G2A) did not confer a significant growth advantage to *P. syringae* pv. cilantro 0788-9 (in a comparison of *P. syringae* pv. cilantro 0788-9 and *P. syringae* pv. cilantro 0788-9 carrying HopZ2, *P* was 0.012; in a comparison of *P. syringae* pv. cilantro 0788-9 and *P. syringae* pv. cilantro 0788-9 carrying HopZ2(G2A), *P* was 0.735; Fisher's PLSD post hoc test), indicating that myristoylation and subse-

quent membrane localization are required for the virulence function of HopZ2. The lack of a virulence function with HopZ2(G2A) was not due to a lack of protein expression because Western blot analysis demonstrated that HopZ2(G2A) was expressed at levels comparable to those of wild-type HopZ2 in *P. syringae* pv. cilantro 0788-9 (see Fig. S1 in the supplemental material). The G2A mutation also had no effect on translocation through the type III secretion system because a chimeric fusion of the full-length HopZ2(G2A) protein to the C terminus of AvrRpt2 (amino acids 80 to 255) (21) induced an HR in *Arabidopsis* (see Fig. S2 in the supplemental material).

DISCUSSION

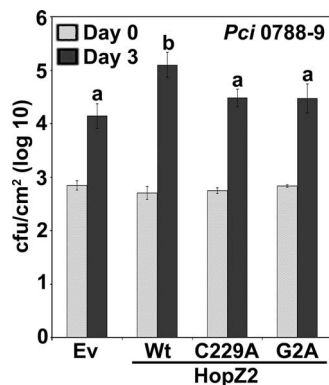The YopJ/HopZ family of type III effectors represents an evolutionarily conserved family of virulence proteins found in

FIG. 6. HopZ2 virulence function in *Arabidopsis* requires an intact myristoylation site. *P. syringae* pv. cilantro 0788-9 (*Pci* 0788-9) carrying the indicated constructs was syringe infiltrated into ecotype Col-0 leaves, and bacterial counts were determined on days 0 and 3. The bacteria (1×10^5 CFU/ml) were syringe infiltrated into the leaves. The error bars indicate 1 standard deviation from the mean. Fisher's PLSD test was used to assess significance. The letters above the bars indicate significance groups. Ev, empty vector; Wt, wild type; C229A, C229A mutant; G2A, G2A mutant.

both plant and animal pathogens. The *P. syringae* HopZ family can be divided into three homology groups, HopZ1, HopZ2, and HopZ3. Three members of the HopZ1 group have been identified, HopZ1a, HopZ1b, and HopZ1c, and the *hopZ1a* allele is most similar to the ancestral allele (37). HopZ1a induces an HR in a number of plants, including *Arabidopsis*. An HR in plants is typically associated with increased resistance to bacterial infection (15). However, there is also at least one example in which a gene-for-gene resistance could be uncoupled from an HR (19). In this study, we further characterized the HopZ1a-induced HR in *Arabidopsis* both qualitatively and quantitatively and demonstrated that the HR is associated with defenses that restrict pathogen growth. In this sense, *hopZ1a* can be classified as an avirulence (*avr*) gene. It has been noted that the timing of the HR induced by different avirulence proteins can vary (52). AvrRpm1 induces a macroscopic HR ~5 h postinfection, whereas AvrRpt2 induces an HR ~21 h postinfection. The timing of the HopZ1a-induced HR is most similar to the timing of an HR induced by AvrRpt2 occurring at ~22 h postinfection.

Like AvrRpt2, HopZ1a possesses a conserved catalytic triad found in cysteine proteases (4, 37). The cysteine protease activity of AvrRpt2 has been demonstrated and requires activation by eukaryotic cyclophilin (14). HopZ1a has also been demonstrated to display protease activity in vitro with the use of a modified casein as a generic substrate (37). This activity was dependent on an intact catalytic cysteine residue and was enhanced by the addition of plant extracts to the reaction mixture (37). However, the activity was weak relative to that of the positive control, trypsin. The weak activity could have been due to the requirement for a eukaryotic cofactor, as suggested by the increase observed with plant extracts. Alternatively, we cannot rule out the possibility that members of the HopZ family may possess acetyltransferase activity similar to that of the *Yersinia pestis* YopJ protein (43, 45). The identification of a specific substrate would undoubtedly confirm the enzymatic activity of the HopZ family. AvrRpt2 displays little or no ac-

tivity in generic protease assays but cleaves the host protein RIN4 at two specific sequences (12, 16, 30). HopZ1a may have a similar substrate specificity, which awaits the identification of *Arabidopsis* target proteins. The identification of host substrates of HopZ1a may also reveal the mode of recognition by its cognate resistance protein since it is becoming apparent that resistance proteins can recognize avirulence proteins through the modifications that they induce in their host targets (15, 66, 67). The resistance protein RPS5 recognizes the type III effector HopAR1 (formerly AvrPphB) via its protease activity on the *Arabidopsis* kinase PBS1 (61). Similarly, the cysteine protease AvrRpt2 degrades its host target protein RIN4, and the disappearance of this protein activates the resistance protein RPS2 (4, 38). The fact that the HopZ1a-induced HR and associated defenses in *Arabidopsis* also require the catalytic cysteine residue C216 indicates that HopZ1a is also recognized indirectly via its enzymatic activity on a host target (Fig. 1 and 2).

The resistance protein responsible for the recognition of HopZ1a in *Arabidopsis* remains to be identified. This recognition is independent of *RPM1*, *RPS2*, *RPS5*, or *RIN4* since plants lacking these genes still display HopZ1a-induced HR (Fig. 3). Recognition is also independent of *RPS4* since HopZ1a restricts bacterial growth in the ecotype RLD background (Fig. 3). Ecotype RLD is a naturally susceptible ecotype which lacks *RPS4* resistance to *P. syringae* pv. tomato DC3000 carrying AvrRps4 (19). Transgenic ecotype RLD expressing the ecotype Col-0 allele of *RPS4* is resistant to DC3000 carrying the *avrRps4* gene (19). Therefore, HopZ1a is recognized in a RIN4-independent manner by a resistance protein other than RPM1, RPS2, RPS5, or RPS4. We are currently identifying the resistance gene responsible for HopZ1a-induced defense responses.

Numerous type III effector proteins possess an N-terminal myristoylation sequence which contributes to membrane localization inside the host cell (41, 46, 53, 60, 64). Interestingly, all of the HopZ family members except HopZ3 possess a predicted N-terminal myristoylation motif with a glycine at the second amino acid position and a cysteine in the first 5 amino acids (Table 2). In HopAR1, the myristoylation sequence is revealed upon autoproteolytic cleavage (46, 64). However, no internal putative myristoylation sequence could be identified in HopZ3, suggesting that this protein is the only family member that is not myristoylated. In support of this, all of the HopZ family members except HopZ3 were predominantly associated with the membrane fraction in assays of transient expression in *N. benthamiana* (Fig. 4). Furthermore, the predicted myristoylation site is required for membrane localization since the G2A mutation resulted in localization predominantly to the soluble fraction in these assays (Fig. 4). The predicted myristoylation sequence is also required for HopZ1a-induced HR (Fig. 5). However, HopZ1a-induced resistance is only partially compromised by the G2A mutation. We speculate that in the absence of myristoylation, some HopZ1a protein is recruited to the membrane fraction, possibly by protein interactions, where it can still partially carry out its biochemical function, ultimately resulting in a compromised, but not eliminated, immune response.

We also identified a novel virulence function for HopZ2 (formerly AvrPpiG), which was originally identified in the pea pathogen *P. syringae* pv. pisi 895A (3). The HopZ2 virulence

function is dependent on both an intact catalytic cysteine (C229) and the predicted myristoylation site. We therefore speculate that myristoylated HopZ2 is membrane localized in *Arabidopsis*, where it acts upon a host protein or proteins, which promotes the virulence of *P. syringae*. HopZ2 is more similar to the AvrBsT, AvrRxv, and AvrXv4 effectors found in the tomato and pepper pathogen *Xanthomonas campestris* and to the PopP1 effector found in the bacterial wilt pathogen *Ralstonia solanacearum* than to the other HopZ proteins (37). AvrRxv and AvrXv4 have been demonstrated to localize to the plant cell cytoplasm, despite possessing putative nuclear localization signals (NLS) (7, 54). AvrBsT also possesses a putative NLS and is predicted to be localized in the nucleus (13). PopP1 does not possess an NLS or a membrane localization sequence and is predicted to localize to the cytosol (32). Therefore, HopZ2 appears to be functionally distinct from these closely related proteins. HopZ2 is more distantly related to XopJ from *X. campestris* pv. vesicatoria 85-10 (37); XopJ was recently demonstrated to be membrane localized and to possess a myristoylation sequence (65). XopJ can also trigger an HR when it is transiently expressed in *N. benthamiana* or *N. clevelandii* (65), but unlike HopZ2, XopJ has not been shown to have a virulence function in plants (47).

Since the membrane localization of HopZ2 does not induce an HR in *Arabidopsis*, the targeted complex may be distinct from the complex targeted by HopZ1a. Alternatively, the same protein(s) may be targeted by HopZ2 and HopZ1a but differentially modified such that only the complex formed by HopZ1a is recognized by the *Arabidopsis* resistance protein. An analogous situation has been found for the *Arabidopsis* protein RIN4, which is differentially modified by at least three distinct type III effector proteins, AvrRpt2, AvrRpm1, and AvrB (4, 38, 39). Determining the host targets of HopZ1a and HopZ2 should help us further understand their avirulence and virulence functions and their effects on host metabolism.

The HopAB family is another evolutionarily diverse and broadly distributed family of *P. syringae* effectors with three closely related homology groups: HopAB1 (including VirPphA), HopAB2 (including AvrPtoB), and HopAB3 (including homologues of AvrPtoB and HopPmaL) (27, 33, 55). Several groups have studied HopAB homologues to determine their virulence and avirulence functions in tomato (33, 34), soybean (26), snap bean (27), and *Arabidopsis* (22); however, this extended family has not been studied from an evolutionary perspective, which limits our understanding of the selective pressures giving rise to this diversity. Since the evolutionary context of the HopZ family is well understood, the HopZ type III effectors provide a unique opportunity to assess the evolutionary pressures driving virulence and avirulence and how these forces drive the underlying molecular and cellular mechanisms of pathogen-host interactions. A key test is to see if HopZ1a confers a virulence function on plants lacking the corresponding resistance gene since both AvrRpt2 and AvrRpm1 can enhance bacterial growth in plants lacking their cognate resistance genes *RPS2* and *RPM1* (10, 21, 51). Furthermore, the identification of *Arabidopsis* targets of the HopZ family of proteins promises to reveal the link between evolutionary and functional diversification. Overall, our results emphasize the significance of genetic diversity among members of this closely related family of type III effector proteins.

REFERENCES

1. **Alfano, J. R., and A. Collmer.** 2004. Type III secretion system effector proteins: double agents in bacterial disease and plant defense. Annu. Rev. Phytopathol. **42:**385–414.
2. **Aoyama, T., and N. H. Chua.** 1997. A glucocorticoid-mediated transcriptional induction system in transgenic plants. Plant J. **11:**605–612.
3. **Arnold, D. L., R. W. Jackson, A. J. Fillingham, S. C. Goss, J. D. Taylor, J. W. Mansfield, and A. Vivian.** 2001. Highly conserved sequences flank avirulence genes: isolation of novel avirulence genes from *Pseudomonas syringae* pv. *pisi*. Microbiology **147:**1171–1182.
4. **Axtell, M. J., S. T. Chisholm, D. Dahlbeck, and B. J. Staskawicz.** 2003. Genetic and molecular evidence that the *Pseudomonas syringae* type III effector protein AvrRpt2 is a cysteine protease. Mol. Microbiol. **49:**1537–1546.
5. **Belkhadir, Y., Z. Nimchuk, D. A. Hubert, D. Mackey, and J. L. Dangl.** 2004. *Arabidopsis* RIN4 negatively regulates disease resistance mediated by RPS2 and RPM1 downstream or independent of the NDR1 signal modulator and is not required for the virulence functions of bacterial type III effectors AvrRpt2 or AvrRpm1. Plant Cell **16:**2822–2835.
6. **Bent, A. F., B. N. Kunkel, D. Dahlbeck, K. L. Brown, R. Schmidt, J. Giraudat, J. Leung, and B. J. Staskawicz.** 1994. *RPS2* of *Arabidopsis thaliana*: a leucine-rich repeat class of plant disease resistance genes. Science **265:**1856–1860.
7. **Bonshtien, A., A. Lev, A. Gibly, P. Debbie, A. Avni, and G. Sessa.** 2005. Molecular properties of the *Xanthomonas* AvrRxv effector and global transcriptional changes determined by its expression in resistant tomato plants. Mol. Plant-Microbe Interact. **18:**300–310.
8. **Boutin, J. A.** 1997. Myristoylation. Cell. Signal. **9:**15–35.
9. **Chang, J. H., A. K. Goel, S. R. Grant, and J. L. Dangl.** 2004. Wake of the flood: ascribing functions to the wave of type III effector proteins of phytopathogenic bacteria. Curr. Opin. Microbiol. **7:**11–18.
10. **Chen, Z. Y., A. P. Kloek, J. Boch, F. Katagiri, and B. N. Kunkel.** 2000. The *Pseudomonas syringae* AvrRpt2 gene product promotes pathogen virulence from inside plant cells. Mol. Plant-Microbe Interact. **13:**1312–1321.
11. **Chisholm, S. T., G. Coaker, B. Day, and B. J. Staskawicz.** 2006. Host-microbe interactions: shaping the evolution of the plant immune response. Cell **124:**803–814.
12. **Chisholm, S. T., D. Dahlbeck, N. Krishnamurthy, B. Day, K. Sjolander, and B. J. Staskawicz.** 2005. Molecular characterization of proteolytic cleavage sites of the *Pseudomonas syringae* effector AvrRpt2. Proc. Natl. Acad. Sci. USA **102:**2087–2092.
13. **Ciesiolka, L. D., T. Hwin, J. D. Gearlds, G. V. Minsavage, R. Saenz, M. Bravo, V. Handley, S. M. Conover, H. Zhang, J. Caporgno, N. B. Phengrasamy, A. O. Toms, R. E. Stall, and M. C. Whalen.** 1999. Regulation of expression of avirulence gene AvrRxv and identification of a family of host interaction factors by sequence analysis of AvrBsT. Mol. Plant-Microbe Interact. **12:**35–44.
14. **Coaker, G., A. Falick, and B. Staskawicz.** 2005. Activation of a phytopathogenic bacterial effector protein by a eukaryotic cyclophilin. Science **308:**548–550.
15. **Dangl, J. L., and J. D. G. Jones.** 2001. Plant pathogens and integrated defence responses to infection. Nature **411:**826–833.
16. **Day, B., D. Dahlbeck, J. Huang, S. T. Chisholm, D. H. Li, and B. J. Staskawicz.** 2005. Molecular basis for the RIN4 negative regulation of RPS2 disease resistance. Plant Cell **17:**1292–1305.
17. **Deng, W. L., A. H. Rehm, A. O. Charkowski, C. M. Rojas, and A. Collmer.** 2003. *Pseudomonas syringae* exchangeable effector loci: sequence diversity in representative pathovars and virulence function in *P. syringae* pv. syringae B728a. J. Bacteriol. **185:**2592–2602.
18. **Espinosa, A., and J. R. Alfano.** 2004. Disabling surveillance: bacterial type III secretion system effectors that suppress innate immunity. Cell. Microbiol. **6:**1027–1040.
19. **Gassmann, W., M. E. Hinsch, and B. J. Staskawicz.** 1999. The *Arabidopsis* RPS4 bacterial resistance gene is a member of the TIR-NBS-LRR family of disease resistance genes. Plant J. **20:**265–277.
20. **Grant, M. R., L. Godiard, E. Straube, T. Ashfield, J. Lewald, A. Sattler, R. W. Innes, and J. L. Dangl.** 1995. Structure of the *Arabidopsis* RPM1 gene enabling dual-specificity disease resistance. Science **269:**843–846.
21. **Guttman, D. S., and J. T. Greenberg.** 2001. Functional analysis of the type III effectors AvrRpt2 and AvrRpm1 of *Pseudomonas syringae* with the use of a

single-copy genomic integration system. Mol. Plant-Microbe Interact. **14:** 145–155.

22. **He, P., L. Shan, N. C. Lin, G. B. Martin, B. Kemmerling, T. Nurnberger, and J. Sheen.** 2006. Specific bacterial suppressors of MAMP signaling upstream of MAPKKK in *Arabidopsis* innate immunity. Cell **125:**563–575.

23. **Heath, M. C.** 2000. Hypersensitive response-related death. Plant Mol. Biol. **44:**321–334.

24. **Huynh, T. V., D. Dahlbeck, and B. J. Staskawicz.** 1989. Bacterial blight of soybean: regulation of a pathogen gene determining host cultivar specificity. Science **245:**1374–1377.

25. **Hwang, M. S. H., R. L. Morgan, S. F. Sarkar, P. W. Wang, and D. S. Guttman.** 2005. Phylogenetic characterization of virulence and resistance phenotypes of *Pseudomonas syringae*. Appl. Environ. Microbiol. **71:**5182–5191.

26. **Jackson, R. W., E. Athanassopoulos, G. Tsiamis, J. W. Mansfield, A. Sesma, D. L. Arnold, M. J. Gibbon, J. Murillo, J. D. Taylor, and A. Vivian.** 1999. Identification of a pathogenicity island, which contains genes for virulence and avirulence, on a large native plasmid in the bean pathogen *Pseudomonas syringae* pathovar *phaseolicola*. Proc. Natl. Acad. Sci. USA **96:**10875–10880.

27. **Jackson, R. W., J. W. Mansfield, H. Ammouneh, L. C. Dutton, B. Wharton, A. Ortiz-Barredo, D. L. Arnold, G. Tsiamis, A. Sesma, D. Butcher, J. Boch, Y. J. Kim, G. B. Martin, S. Tegli, J. Murillo, and A. Vivian.** 2002. Location and activity of members of a family of VirPphA homologues in pathovars of *Pseudomonas syringae* and *P. savastanoi*. Mol. Plant Pathol. **3:**205–216.

28. **Jones, J. D. G., and J. L. Dangl.** 2006. The plant immune system. Nature **444:**323–329.

29. **Katagiri, F., R. Thilmony, and S. Y. He.** 2002. The *Arabidopsis thaliana-Pseudomonas syringae* interaction, p. 1–35. *In* C. R. Somerville and E. M. Meyerowitz (ed.), The Arabidopsis book. American Society of Plant Biologists, Rockville, MD.

30. **Kim, H. S., D. Desveaux, A. U. Singer, P. Patel, J. Sondek, and J. L. Dangl.** 2005. The *Pseudomonas syringae* effector AvrRpt2 cleaves its C-terminally acylated target, RIN4, from *Arabidopsis* membranes to block RPM1 activation. Proc. Natl. Acad. Sci. USA **102:**6496–6501.

31. **Koch, E., and A. Slusarenko.** 1990. *Arabidopsis* is susceptible to infection by a downy mildew fungus. Plant Cell **2:**437–445.

32. **Lavie, M., E. Shillington, C. Eguiluz, N. Grimsley, and C. Boucher.** 2002. PopP1, a new member of the YopJ/AvrRxv family of type III effector proteins, acts as a host-specificity factor and modulates aggressiveness of *Ralstonia solanacearum*. Mol. Plant-Microbe Interact. **15:**1058–1068.

33. **Lin, N. C., R. B. Abramovitch, Y. J. Kim, and G. B. Martin.** 2006. Diverse AvrPtoB homologs from several *Pseudomonas syringae* pathovars elicit Pto-dependent resistance and have similar virulence activities. Appl. Environ. Microbiol. **72:**702–712.

34. **Lin, N. C., and G. B. Martin.** 2007. Pto- and Prf-mediated recognition of AvrPto and AvrPtoB restricts the ability of diverse *Pseudomonas syringae* pathovars to infect tomato. Mol. Plant-Microbe Interact. **20:**806–815.

35. **Lindeberg, M., J. Stavrinides, J. H. Chang, J. R. Alfano, A. Collmer, J. L. Dangl, J. T. Greenberg, J. W. Mansfield, and D. S. Guttman.** 2005. Proposed guidelines for a unified nomenclature and phylogenetic analysis of type III Hop effector proteins in the plant pathogen *Pseudomonas syringae*. Mol. Plant-Microbe Interact. **18:**275–282.

36. **Link, A. J., D. Phillips, and G. M. Church.** 1997. Methods for generating precise deletions and insertions in the genome of wild-type *Escherichia coli*: application to open reading frame characterization. J. Bacteriol. **179:**6228–6237.

37. **Ma, W. B., F. F. T. Dong, J. Stavrinides, and D. S. Guttman.** 2006. Type III effector diversification via both pathoadaptation and horizontal transfer in response to a coevolutionary arms race. PLOS Genet. **2:**2131–2142.

38. **Mackey, D., Y. Belkhadir, J. M. Alonso, J. R. Ecker, and J. L. Dangl.** 2003. *Arabidopsis* RIN4 is a target of the type III virulence effector AvrRpt2 and modulates RPS2-mediated resistance. Cell **112:**379–389.

39. **Mackey, D., B. F. Holt, A. Wiig, and J. L. Dangl.** 2002. RIN4 interacts with *Pseudomonas syringae* type III effector molecules and is required for RPM1-mediated resistance in *Arabidopsis*. Cell **108:**743–754.

40. **Martin, G. B., A. J. Bogdanove, and G. Sessa.** 2003. Understanding the functions of plant disease resistance proteins. Annu. Rev. Plant Biol. **54:**23–61.

41. **Maurer-Stroh, S., and F. Eisenhaber.** 2004. Myristoylation of viral and bacterial proteins. Trends Microbiol. **12:**178–185.

42. **Mindrinos, M., F. Katagiri, G. L. Yu, and F. M. Ausubel.** 1994. The *A. thaliana* disease resistance gene *RPS2* encodes a protein containing a nucleotide-binding site and leucine-rich repeats. Cell **78:**1089–1099.

43. **Mittal, R., S. Y. Peak-Chew, and H. T. McMahon.** 2006. Acetylation of MEK2 and I kappa B kinase (IKK) activation loop residues by YopJ inhibits signaling. Proc. Natl. Acad. Sci. USA **103:**18574–18579.

44. **Mudgett, M. B., and B. J. Staskawicz.** 1999. Characterization of the *Pseudomonas syringae* pv. *tomato* AvrRpt2 protein: demonstration of secretion and processing during bacterial pathogenesis. Mol. Microbiol. **32:**927–941.

45. **Mukherjee, S., G. Keitany, Y. Li, Y. Wang, H. L. Ball, E. J. Goldsmith, and K. Orth.** 2006. *Yersinia* YopJ acetylates and inhibits kinase activation by blocking phosphorylation. Science **312:**1211–1214.

46. **Nimchuk, Z., E. Marois, S. Kjemtrup, R. T. Leister, F. Katagiri, and J. L. Dangl.** 2000. Eukaryotic fatty acylation drives plasma membrane targeting and enhances function of several type III effector proteins from *Pseudomonas syringae*. Cell **101:**353–363.

47. **Noel, L., F. Thieme, J. Gabler, D. Buttner, and U. Bonas.** 2003. XopC and XopJ, two novel type III effector proteins from *Xanthomonas campestris* pv. vesicatoria. J. Bacteriol. **185:**7092–7102.

48. **Orth, K., L. E. Palmer, Z. Q. Bao, S. Stewart, A. E. Rudolph, J. B. Bliska, and J. E. Dixon.** 1999. Inhibition of the mitogen-activated protein kinase kinase superfamily by a *Yersinia* effector. Science **285:**1920–1923.

49. **Orth, K., Z. H. Xu, M. B. Mudgett, Z. Q. Bao, L. E. Palmer, J. B. Bliska, W. F. Mangel, B. Staskawicz, and J. E. Dixon.** 2000. Disruption of signaling by *Yersinia* effector YopJ, a ubiquitin-like protein protease. Science **290:** 1594–1597.

50. **Puri, N., C. Jenner, M. Bennett, R. Stewart, J. Mansfield, N. Lyons, and J. Taylor.** 1997. Expression of *avrPphB*, an avirulence gene from *Pseudomonas syringae* pv. *phaseolicola*, and the delivery of signals causing the hypersensitive reaction in bean. Mol. Plant-Microbe Interact. **10:**247–256.

51. **Ritter, C., and J. L. Dangl.** 1995. The *avrRpm1* gene of *Pseudomonas syringae* pv. *maculicola* is required for virulence on *Arabidopsis*. Mol. Plant-Microbe Interact. **8:**444–453.

52. **Ritter, C., and J. L. Dangl.** 1996. Interference between two specific pathogen recognition events mediated by distinct plant disease resistance genes. Plant Cell **8:**251–257.

53. **Robert-Seilaniantz, A., L. B. Shan, J. M. Zhou, and X. Y. Tang.** 2006. The *Pseudomonas syringae* pv. *tomato* DC3000 type III effector HopF2 has a putative myristoylation site required for its avirulence and virulence functions. Mol. Plant-Microbe Interact. **19:**130–138.

54. **Roden, J., L. Eardley, A. Hotson, Y. Y. Cao, and M. B. Mudgett.** 2004. Characterization of the *Xanthomonas* AvrXv4 effector, a SUMO protease translocated into plant cells. Mol. Plant-Microbe Interact. **17:**633–643.

55. **Sarkar, S. F., J. S. Gordon, G. B. Martin, and D. S. Guttman.** 2006. Comparative genomics of host-specific virulence in *Pseudomonas syringae*. Genetics **174:**1041–1056.

56. **Sarkar, S. F., and D. S. Guttman.** 2004. Evolution of the core genome of *Pseudomonas syringae*, a highly clonal, endemic plant pathogen. Appl. Environ. Microbiol. **70:**1999–2012.

57. **Schornack, S., A. Meyer, P. Romer, T. Jordan, and T. Lahaye.** 2006. Gene-for-gene-mediated recognition of nuclear-targeted AvrBs3-like bacterial effector proteins. J. Plant Physiol. **163:**256–272.

58. **Schweizer, H. P., T. Klassen, and T. Hoang.** 1996. Improved methods for gene analysis and expression in *Pseudomonas* spp., p. 229–237. *In* T. Nakazawa, K. Furukawa, D. Haas, and S. Silver (ed.), Molecular biology of pseudomonads. ASM Press, Washington, DC.

59. **Sessa, G., M. D'Ascenzo, and G. B. Martin.** 2000. Thr38 and Ser198 are Pto autophosphorylation sites required for the AvrPto-Pto-mediated hypersensitive response. EMBO J. **19:**2257–2269.

60. **Shan, L. B., V. K. Thara, G. B. Martin, J. M. Zhou, and X. Y. Tang.** 2000. The *Pseudomonas* AvrPto protein is differentially recognized by tomato and tobacco and is localized to the plant plasma membrane. Plant Cell **12:**2323–2337.

61. **Shao, F., C. Golstein, J. Ade, M. Stoutemyer, J. E. Dixon, and R. W. Innes.** 2003. Cleavage of *Arabidopsis* PBS1 by a bacterial type III effector. Science **301:**1230–1233.

62. **Simonich, M. T., and R. W. Innes.** 1995. A disease resistance gene in *Arabidopsis* with specificity for the *avrPph3* gene of *Pseudomonas syringae* pv. *phaseolicola*. Mol. Plant-Microbe Interact. **8:**637–640.

63. **Tamaki, S., D. Dahlbeck, B. Staskawicz, and N. T. Keen.** 1988. Characterization and expression of two avirulence genes cloned from *Pseudomonas syringae* pv. *glycinea*. J. Bacteriol. **70:**4846–4854.

64. **Tampakaki, A. P., M. Bastaki, J. W. Mansfield, and N. J. Panopoulos.** 2002. Molecular determinants required for the avirulence function of AvrPphB in bean and other plants. Mol. Plant-Microbe Interact. **15:**292–300.

65. **Thieme, F., R. Szczesny, A. Urban, O. Kirchner, G. Hause, and U. Bonas.** 2007. New type III effectors from *Xanthomonas campestris* pv. *vesicatoria* trigger plant reactions dependent on a conserved N-myristoylation motif. Mol. Plant-Microbe Interact. **20:**1250–1261.

66. **van der Biezen, E. A., and J. D. G. Jones.** 1998. Plant disease resistance proteins and the gene-for-gene concept. Trends Biochem. Sci. **23:**454–456.

67. **Van der Hoorn, R. A. L., P. De Wit, and M. Joosten.** 2002. Balancing selection favors guarding resistance proteins. Trends Plant Sci. **7:**67–71.

68. **Vinatzer, B. A., G. M. Teitzel, M. W. Lee, J. Jelenska, S. Hotton, K. Fairfax, J. Jenrette, and J. T. Greenberg.** 2006. The type III effector repertoire of *Pseudomonas syringae* pv. *syringae* B728a and its role in survival and disease on host and nonhost plants. Mol. Microbiol. **62:**26–44.